JOURNAL OF CATALYSIS 135, 135–146 (1992)

Encapsulation of Molecular Hydrogen in Ion-Exchanged A Zeolites at 1 atm

ANGELOS M. EFSTATHIOU,* ERIC V.R. BORGSTEDT,† STEVEN L. SUIB,*,†,[1] AND CARROLL O. BENNETT*

*Department of Chemical Engineering and †Department of Chemistry, University of Connecticut, Storrs, Connecticut 06269-3060

Received April 26, 1991; revised December 23, 1991

About 1.5 and 2.0 μmol/g of molecular H_2 is encapsulated in the sodalite and supercages, respectively, of NaA zeolite at 1 atm H_2 pressure and temperatures higher than 200°C. At 37°C and 1 atm H_2 pressure, encapsulation of molecular H_2 occurs only in the supercages. For these conditions, equilibrium (2.3 μmol/g) is obtained only after 24 h of sorption in H_2 flow. The site of encapsulation of H_2 is probed by exchanging Cs^+, Ni^{2+}, and Eu^{3+} for Na^+ cations into the supercage, near the six-membered oxygen window, and sodalite cage, respectively, of zeolite A. The removal of H_2 encapsulated in NaA can be studied by programming the temperature in 1 atm Ar gas flow. This method provides an apparent activation energy for diffusion of 26.0 and 11.5 kcal/mol for the H_2 encapsulated in the sodalite and supercages, respectively, of NaA zeolite. Diffusivities of H_2 for NaA and Eu/NaA zeolites have been determined from isothermal uptake data.

INTRODUCTION

We have recently presented results on encapsulation of molecular H_2 at 1 atm H_2 pressure in the range 37–150°C in NaX zeolite (*1*). The quantities observed (1.0–2.5 μmol/g) could be measured accurately by temperature-programmed diffusion (TP-Diff) methods with on-line mass spectrometry. Exchanging Cs^+, Ni^{2+}, and Eu^{3+} for Na^+ cations into the supercages, hexagonal prisms, and sodalite cages, respectively, of X zeolite led to the conclusion that H_2 is trapped in the sodalite cages of X zeolite (*1*).

Encapsulation of molecular H_2 in NaA and alkali cation (K, Rb, Cs) exchanged zeolites A has been studied (*2–5*) at H_2 pressures in the range 120–134 atm. In the case of NaA it was found that H_2 is encapsulated in the β-cage (via molecular jumps through six-membered windows), whereas in other alkali-exchanged A zeolites, H_2 is encapsulated in the α-cage (via molecular jumps through a varying effective eight-membered window). The effect of degree of exchange of alkali cation on the amount of H_2 encapsulation and the apparent activation energy for diffusion of H_2 out of the zeolite were also probed (*5*). For example, it has been suggested (*5*) that encapsulation of H_2 occurs in both α-cages (supercage) and β-cages (sodalite) of zeolite A when there are more than 2.3 Cs^+ cations per unit cell. Below this level of ion-exchange encapsulation has been suggested to be restricted to the β-cage (sodalite) (*5*).

In the present work we report results for H_2 encapsulation at 1 atm H_2 pressure and 37–300°C in NaA, Cs/NaA, Ni/NaA, and Eu/NaA zeolites. The results for these zeolites suggest that there are two sites for H_2 encapsulation of NaA. The population of these two sites by H_2 depends on the type of cation in the zeolite and the temperature of sorption. To our knowledge, H_2 encapsulation at 1 atm H_2 pressure in various ion-exchanged zeolite A materials has not been previously studied. Rationale for these experiments is to probe cation location and

[1] To whom correspondence should be addressed.

0021-9517/92 $3.00

hydrogen diffusivity under conditions normally used in the laboratory.

EXPERIMENTAL

Preparation of zeolites. Linde NaA zeolite (4A, 600 mesh) was purchased from Alfa Ventron Corp. (Danvers, MA) and used without further purification. The crystal size was about 1.2 μm as determined by scanning electron microscopy. This zeolite was ion-exchanged by taking 1 g of zeolite and stirring this for 18 h in a round-bottom flask with 0.05 *M* solutions of Eu^{3+}, Ni^{2+}, and Cs^+ cations. $EuCl_3 \cdot 6H_2O$, $CsCl \cdot 6H_2O$ and $NiCl_2 \cdot 6H_2O$ salts purchased from Alfa Ventron were used for these solutions. Samples were filtered, washed with distilled deionized water, and dried under vacuum as previously described (*6*). The approximate formulas of the exchanged zeolites are $Eu_{3.2}Na_{2.4}A$, $Cs_{2.6}Na_{9.4}A$, and $Ni_{2.4}Na_{7.2}A$. All zeolite samples were dehydrated under vacuum prior to sorption experiments as previously described (*1*). Loading procedures of the zeolite into the reactor under inert atmosphere have been described (*1*). The zeolite bed (0.50–1.2 g powder) was supported by fine stainless-steel screens and glass wool.

Characterization of zeolites. The degree of ion-exchange in the present zeolites has been measured by atomic absorption. The crystallinity of the samples after ion-exchange and TPDiff studies was examined with X-ray powder diffraction (XRD) as previously described (*7*). XRD results for the ion-exchanged, dehydrated, and treated (after sorption and TPDiff experiments) zeolites show that the samples all retained their structures with no loss of crystallinity.

Reactor flow system. The once-through stainless-steel microreactor (3.0 mL) and the flow system used have previously been described (*8*). Air exposure of the zeolite sample during transfer and installation in the flow-panel has been avoided (*1*). H_2 sorption experiments were performed with 1 atm H_2 pressure. Argon was used as carrier gas in the temperature-programmed diffusion (TPDiff) studies. Purification of H_2 and Ar gases has been described (*8*). The flow rate of all gases used was 30 mL/min (ambient).

Mass spectrometry. After appropriate tune-up of the high resolution mass spectrometer (Nuclide 12-90-G), a flat-topped peak for mass number (*m/e*) 2 (H_2^+ ion) was obtained, avoiding falsification of results from reasonable drifts in the magnetic and/or electrostatic fields. Data acquisition and calibration and integration of the mass spectrometer response have been described (*1*). The detection limit for H_2 was about 2 ppm. The contribution of H_2O to the *m/e* = 2 signal was estimated to be less than 0.5%.

RESULTS

(A) H_2 Encapsulation in Zeolite NaA

Diffusion of H_2 out of dehydrated NaA following sorption at 37°C. Before the start of a sorption experiment, zeolite samples were checked *in situ* for residual water at 400°C by mass spectrometry. After the response of water (if present) reached the baseline, the reactor was closed off and cooled to the sorption temperature.

Figure 1 presents diffusion results obtained for various initial amounts of sorbed (encapsulated) H_2. Sorption at 37°C and 1 atm H_2 pressure was performed with 1.06 g

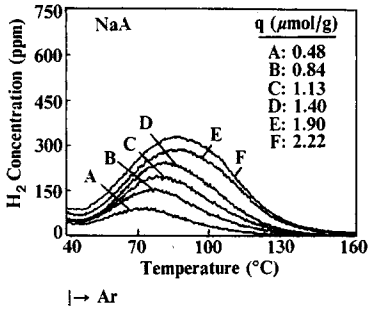

FIG. 1. TPDiff experiment for measuring H_2 encapsulation into NaA. Experimental procedure: H_2(1 atm, 37°C, Δt) → Ar(180 s), 37°C → TPDiff (β = 10°C/min). Amounts of encapsulation, *q*, corresponding to a given time on H_2 stream, Δt, are shown in Table 1. Amount of sample used 1.06 g, flow rate 30 mL/min (ambient).

TABLE 1

Hydrogen Encapsulation vs Time in NaA Zeolite (T = 37°C, P_{H_2} = 1 atm)

Time	H_2 uptake (μmol/g)[a]	T_M(°C)[b]
20 min	0.48	72
1 h	0.84	76
2 h	1.13	78
4 h	1.40	81
5 h	1.72	84
12 h	1.90	86
18 h	2.22	86
24 h	2.38	86

[a] 1 μmol/g = 0.003 molecules/unit cell.
[b] Peak maximum temperature.

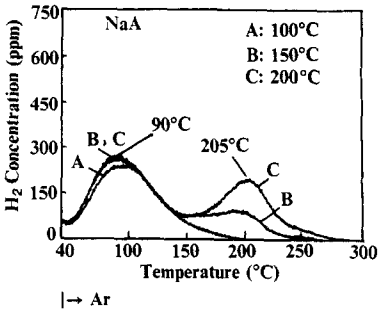

FIG. 2. TPDiff experiment for measuring H_2 encapsulation into NaA. Experimental procedure: H_2(1 atm, T, 1 h) → cool in H_2 to 37°C → Ar(180 s), 37°C → TPDiff (β = 10°C/min). Curve (A) T = 100°C; curve (B) T = 150°C; curve (C) T = 200°C. Amount of sample used 1.06 g, flow rate 30 mL/min (ambient).

of dehydrated NaA zeolite. The time on H_2 stream required to obtain the different amounts of encapsulation shown in Fig. 1 is given in Table 1. The diffusion (decapsulation) process of H_2 was performed under 1 atm Ar gas flow by programming the temperature at the rate of 10°C/min. Before the initiation of any temperature-programmed diffusion (TPDiff) run, the gas-phase reactor volume was purged with Ar for 180 s at 37°C. This procedure ensured the complete removal of gas-phase H_2. At 37°C some H_2 encapsulated in the zeolite diffuses away from the zeolite crystal and is measured (Fig. 1). The rate of diffusion is increased as temperature increases, and a maximum in the rate occurs. The corresponding maximum temperature (T_M) for each case in Fig. 1 is given in Table 1. This T_M is found to increase with increasing initial amount of H_2 encapsulated in the zeolite for up to about 2.0 μmol/g. Curve (F) in Fig. 1 represents the TPDiff response of an equilibrium amount of H_2 encapsulation.

Diffusion of H_2 out of dehydrated NaA following sorption in the range 100–300°C. The effect of sorption temperature on the amount of H_2 encapsulation in NaA is presented in Fig. 2. Curves (A), (B), and (C) give the diffusion response of H_2 after sorption with 1 atm H_2 for 1 h at 100, 150, and 200°C, respectively. Following sorption the reactor is cooled in H_2 to 37°C before the TPDiff. At temperatures of sorption of about 200°C, a second peak (peak 2) in the TPDiff spectrum of Fig. 2 appears with T_M at 205°C for all sorption temperatures studied which was not observed in Fig. 1. This peak grows with sorption temperature in the range 100–200°C, whereas at higher temperatures (300°C) no further growth is observed. On increasing the time of sorption to 2 h the same result as for that after 1 h of sorption is obtained. On the other hand, the first peak (peak 1, T_M = 90°C) does not grow with increasing temperature of sorption. An approximate deconvolution of the TPDiff response in Fig. 2 provides the quantities of encapsulated H_2 corresponding to these two peaks, and these are given in Table 2.

TABLE 2

Hydrogen Encapsulation vs Temperature in NaA Zeolite: H_2(1 atm, T, 1 h) → cool in H_2 to 37°C → Ar(180 s) → TPDiff

T(°C)	H_2 uptake (μmol/g)[a]		
	Peak 1	Peak 2	Total
100	1.88	0.10	1.98
150	2.07	0.68	2.75
200	2.03	1.40	3.43
300	2.00	1.50	3.50

[a] 1 μmol/g = 0.003 molecules/unit cell.

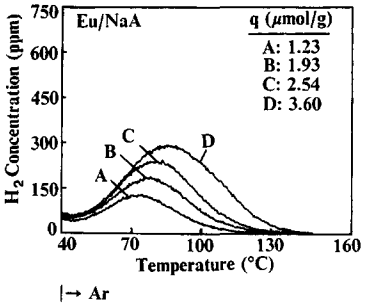

FIG. 3. TPDiff experiment for measuring H_2 encapsulation into Eu/NaA. Experimental procedure: H_2 (1 atm, 37°C, Δt) → Ar(180 s), 37°C → TPDiff (β = 10°C/min). Amounts of encapsulation, q, corresponding to a given time on H_2 stream, Δt, are shown in Table 3. Amount of sample used 0.50 g, flow rate 30 mL/min (ambient).

TABLE 3

Hydrogen Encapsulation vs Time in Eu/NaA Zeolite (T = 37°C, P_{H_2} = 1 atm)[a]

Time	H_2 uptake (μmol/g)[b]	T_M(°C)[c]
12 min	0.85	
20 min	1.23	72
40 min	1.61	
1 h	1.93	75
2 h	2.54	79
3.2 h	2.78	
12.5 h	3.45	
18 h	3.60	85
24 h	3.70	

[a] For sorption temperatures in the range 100–300°C, no H_2 uptake (2nd peak) was observed.
[b] 1 μmol/g = 0.003 molecules/unit cell.
[c] Peak maximum temperature.

(B) *H_2 Encapsulation in Ion-Exchanged NaA Zeolites*

Diffusion of H_2 out of dehydrated Eu/NaA following sorption in the range 37–300°C. In order to probe the site of H_2 encapsulation and the results obtained in Figs. 1 and 2 with NaA, exchange with Eu^{3+}, Cs^+, and Ni^{2+} cations was done, and similar sorption and TPDiff experiments as those with NaA (Figs. 1 and 2) were repeated by using 0.5-g samples.

Diffusion results of encapsulated H_2 in Eu/NaA for various initial sorption amounts are given in Fig. 3 and Table 3 for sorption at 37°C. The qualitative features of these TPDiffs are very similar to those obtained with NaA for the same initial uptake (i.e., compare curve (B) in Fig. 3 with curve (E) in Fig. 1). Of interest are the higher quantities obtained with Eu/NaA than NaA at the same experimental conditions. This behavior is discussed later. On increasing the sorption temperature from 100 to 300°C, and performing the same experiments as for NaA (Fig. 2), no second TPDiff peak has been observed.

Diffusion of H_2 out of dehydrated Cs/NaA following sorption in the range 37–300°C. TPDiff results of encapsulated H_2 in Cs/NaA for various sorption conditions are given in Fig. 4. Curve (A) corresponds to sorption at 37°C for 3 h on H_2 stream, curve (B) to sorption at 37°C for 18 h on H_2 stream, and curve (C) to sorption at 200°C for 1 h on H_2 stream followed by cooling of the reactor in H_2 flow to 37°C. The quantities of H_2 encapsulation obtained are: 1.00, 1.32, and 4.15 μmol/g for curves (A), (B), and (C), respectively. Sorption at 300°C for 1 h followed by cooling of the reactor in H_2 flow to 37°C produces essentially the same result as of Fig. 4, curve (C).

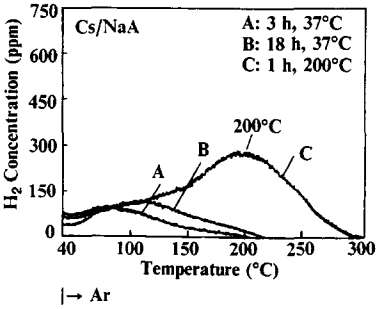

FIG. 4. TPDiff experiment for measuring H_2 encapsulation into Cs/NaA. Experimental procedure: H_2(1 atm, T, 1 h) → cool in H_2 to 37°C → Ar(180 s), 37°C → TPDiff (β = 10°C/min). Curve (A) T = 37°C, Δt = 3 h; curve (B) T = 37°C, Δt = 18 h; curve (C) T = 200°C, Δt = 1 h. Amount of sample used 0.50 g, flow rate 30 mL/min (ambient).

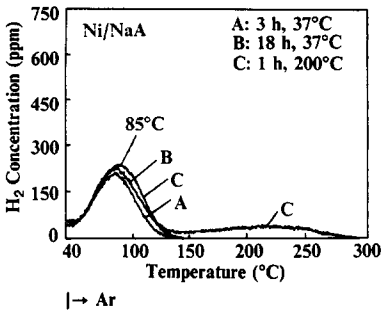

FIG. 5. TPDiff experiment for measuring H_2 encapsulation into Ni/NaA. Experimental procedure: H_2(1 atm, T, 1 h) → cool in H_2 to 37°C → Ar(180 s), 37°C → TPDiff (β = 10°C/min). Curve (A) T = 37°C, Δt = 3 h; curve (B) T = 37°C, Δt = 18 h; curve (C) T = 200°C, Δt = 1 h. Amount of sample used 0.50 g, flow rate 30 mL/min (ambient).

Diffusion of H_2 out of dehydrated Ni/NaA following sorption in the range 37–200°C. TPDiff results of encapsulated H_2 in Ni/NaA for the same conditions as for Cs/NaA (Fig. 4) are given in Fig. 5. The quantities of H_2 encapsulation obtained are: 1.06, 1.28, and 1.70 μmol/g for curves (A), (B), and (C), respectively. Note that the second peak in Fig. 5, curve (C), is largely reduced (0.35 μmol/g) compared to that in Fig. 4, curve (C), and Fig. 2, curve (C) (1.4 μmol/g) for Cs/NaA and NaA zeolites, respectively. On the other hand, the first peak in Fig. 5 grows slightly with increasing temperature of sorption, a result opposite to that for Cs/NaA (Fig. 4), but similar to that for NaA (Fig. 2). Note that the T_M of the first peak in Fig. 5 remains the same (T_M = 85°C) for all the cases in Fig. 5.

(C) *Kinetics of Decapsulation*

For the present work, the removal of encapsulated H_2, when the H_2 pressure is released (Figs. 1–5), is controlled by a diffusion process. Diffusivities can then be calculated based on the following relationship.

$$D(t) = D_o \exp(-E/RT(t)), \quad (1)$$

where $D(t)$ is the diffusivity (cm^2/s) at time t and temperature $T(t)$, E (kcal/mol) is the activation energy for diffusion of H_2, and D_o (cm^2/s) is the limiting diffusivity. An analysis for this case has been presented (*3, 9*), where the following equation is used:

$$\ln(T_M^2/\beta) = E/RT_M + \ln(E\alpha^2/1.5\pi^2 RD_o). \quad (2)$$

By varying the heating rate (β), the peak maximum temperature (T_M) is expected to vary, and by plotting the left-hand side of Eq. (2) against $1/T_M$ a straight line is expected. The parameter α represents the radius of an assumed spherical crystallite. From this plot E and D_o can be calculated.

Figure 6 gives the TPDiff spectrum obtained using a heating rate β = 14.5°C/min. The effect of β on the T_M for both peaks is clearly shown when these results are compared to those of Fig. 2, curve (C), obtained with β = 10°C/min. For heating rates varied in the range 10–25°C/min, activation energies of E_1 = 11.5 and E_2 = 26.0 kcal/mol are obtained, which correspond to the first peak (T_M = 100°C) and the second peak (T_M = 213°C) in Fig. 6, respectively. The corresponding values of D_o/α^2 are 3.1 × 10^3 s^{-1} and 2.9 × 10^8 s^{-1}.

Similar experiments as of Fig. 6 were performed with Eu/NaA zeolite after sorption at 37°C and for an initial amount of H_2 encapsulated 1.93 μmol/g (Fig. 3, curve (B)). An activation energy of E = 9.1 kcal/

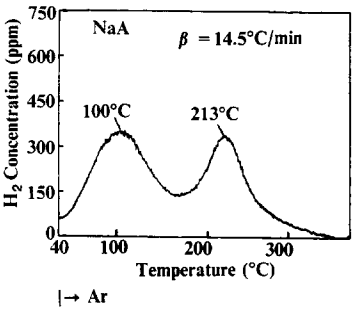

FIG. 6. Effect of heating rate, β, on the peak maximum temperature, T_M, of TPDiff. Experimental procedure: H_2(1 atm, 200°C, 1 h) → cool in H_2 to 37°C → Ar(180 s), 37°C → TPDiff (β = 14.5°C/min). Effect of β on the T_M is seen by comparing these results to those in Fig. 2, curve (C).

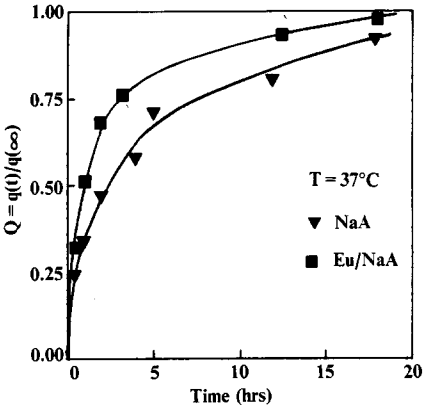

FIG. 7. Diffusion uptake of H_2 vs time by NaA and Eu/NaA zeolites. The amount of diffusion (encapsulation) was determined according to the sequence: H_2(1 atm, 37°C, Δt) → Ar(180 s), 37°C → TPDiff (β = 10°C/min). Amount of sample used: NaA = 1.06 g; Eu/NaA = 0.50 g.

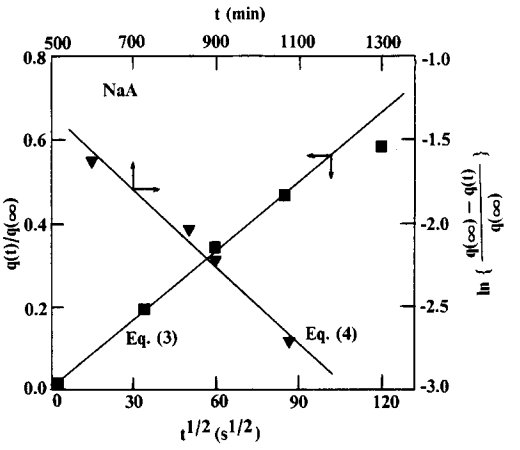

FIG. 8. Determination of D/α^2 (s^{-1}) for NaA zeolite according to Eqs. (3) and (4) in the text; T = 37°C.

mol and a value of $D_o/\alpha^2 = 1.9 \times 10^2\ s^{-1}$ are found.

(D) Kinetics of Isothermal Encapsulation

The decapsulation results of Figs. 1 and 3 for NaA and Eu/NaA are plotted in Fig. 7 as dimensionless uptake $Q(t) = q(t)/q(\infty)$ vs time, where $q(t)$ is the uptake at time t, and $q(\infty)$ is the uptake at equilibrium conditions. For any given sorption time the rate of sorption of H_2 in Eu/NaA is higher than in NaA, and this behavior is discussed later. The curves in Fig. 7 can now be interpreted to obtain diffusion parameters which control the sorption (encapsulation) at 37°C and 1 atm H_2 pressure. Since the uptake of H_2 is so small (see Tables 1 and 3), it is appropriate to use the classical solution of the diffusion problem for a sphere at constant temperature and subjected to a constant gas concentration starting at time zero. The exact analytical solution has been given (*10, 11*). It has been shown, however, that for small values of time, t, it is sufficient to describe the diffusion process (within this time) by the following equation (*27*).

$$\frac{q(t) - q(0)}{q(\infty) - q(0)} = 6(D/\pi\alpha^2)^{1/2}t^{1/2} \qquad (3)$$

where $q(0)$ is the uptake before sorption starts (time 0). For large values of t the following equation is appropriate:

$$\ln\left\{\frac{q(\infty) - q(t)}{q(\infty) - q(0)}\right\} = \ln(6/\pi^2) - (D\pi^2/\alpha^2)t. \qquad (4)$$

Figures 8 and 9 present results obtained after using Eqs. (3) and (4) to calculate the H_2 diffusivity (D/α^2) from isothermal sorption measurements. For the case of NaA (Fig. 8) and for short times ($t \leq 2$ h), a very good fit according to Eq. (3) is obtained. For $t \geq 4$ h a deviation from Eq. (3) is ap-

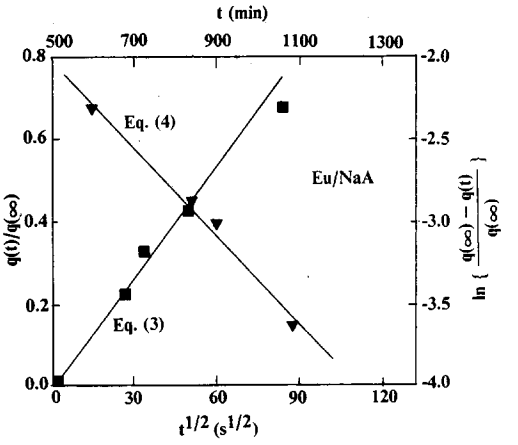

FIG. 9. Determination of D/α^2 (s^{-1}) for Eu/NaA zeolite according to Eqs. (3) and (4) in the text; T = 37°C.

parent, and this is also shown in Fig. (8). A value of $D/\alpha^2 = 2.6 \times 10^{-6}$ s^{-1} is obtained by Eq. (3), compared to 3.8×10^{-6} s^{-1} obtained by Eq. (4) for H_2 diffusion in NaA. For the case of H_2 diffusion in Eu/NaA (Fig. 9), a value of $D/\alpha^2 = 6.3 \times 10^{-6}$ s^{-1} is obtained by Eq. (3), compared to 4.6×10^{-6} s^{-1} obtained by Eq. (4).

DISCUSSION

(A) *H_2 Encapsulation in NaA and Eu/NaA Zeolites*

The small quantities of H_2 uptake in NaA and the other ion-exchanged A zeolites were the result of an encapsulation and not of any other process, such as adsorption on metallic impurities, sorption on the steel walls of reactor, or spillover. Similar blank experiments as those reported for H_2 encapsulation in NaX (*1*) were performed, and the results obtained confirm the interpretation given above. In addition, the absence of a second H_2 TPDiff peak following sorption at 200°C in Eu/NaA, a result opposite that found for NaA (Fig. 2, curve (C)), is strong evidence that the present results are consistent with an H_2 encapsulation phenomenon.

In our recent study of H_2 encapsulation at 37°C and 1 atm H_2 in $Eu_{25}Na_{11}X$ zeolite (*1*), exchange of Eu^{3+} for Na^+ resulted in complete suppression of encapsulation of H_2. We proposed that the bulky ion Eu_4O^{+10} that formed in the sodalite cage of X zeolite (after dehydration of 400°C) prevented all encapsulation in the sodalite cage. In the present work a similar result is obtained for NaA zeolite but after sorption of H_2 at temperatures higher than 100°C (Fig. 2, Tables 2 and 3).

The second H_2 TPDiff peak (T_M = 205°) in Fig. 2 with NaA was totally eliminated in the case of Eu/NaA zeolite. This result suggests that europium ion(s) blocked passage of H_2 through the six-membered ring into the sodalite cage, or H_2 sorption in the same cage. Luminescence lifetime (*6*), extended X-ray absorption fine structure (EXAFS) (*6*), electron paramagnetic resonance (*28*), and Mössbauer data (*29*) support the formation of Eu_4O^{+10} species in A zeolite. Evidence for the presence of Eu^{3+} in the sodalite cage of dehydrated zeolites X and Y has also been given (*12, 13*) consistent with the Eu_4O^{10+} species. What remains to be explained is the higher sorption temperature required for H_2 to pass through the six-membered ring into the sodalite cage of zeolite A than that of zeolite X.

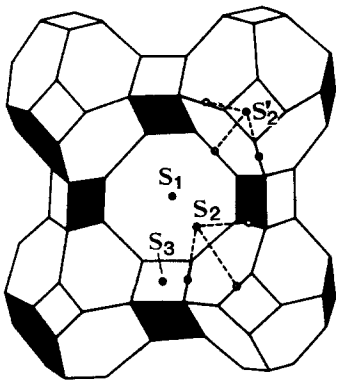

FIG. 10. Cation sites of dehydrated zeolite A.

Figure 10 gives the crystal structure of zeolite A with site assignments that are needed to better understand results of the present work. It is generally agreed (*14*) that in dehydrated NaA and for one unit cell, 8 Na^+ ions occupy S_2 sites (at the centers of six-membered rings displaced into the supercage, α-cage), 3 Na^+ occupy S_1 sites (at the centers of the eight-membered rings displaced into the α-cage), and 1 Na^+ occupies the S_3' site (on a twofold axis opposite a four-membered ring into the α-cage). In dehydrated NaX zeolite and for one unit cell, 16 Na^+ ions occupy site I (in the center of hexagonal prism), 32 Na^+ occupy site II (on the six-membered ring, unjoined hexagonal face), and 48 Na^+ occupy site III (on the walls of the channels) (*14*). Molecular hydrogen is expected to enter the sodalite cage only through the six-membered rings. The positions of Na^+ ions near this ring may, therefore, play a key role for the passage of H_2 through this ring.

Some difference between NaA and NaX has been reported for the distance of Na^+

ions from the center of the six-membered rings (0.4 Å in NaA vs 0.6 Å in NaX) (*15, 16*). On the other hand, a different Na^+ ion mobility around the six-membered ring in NaX and NaA might be considered as an important factor that may explain the present H_2 encapsulation results obtained with NaA and Eu/NaA zeolites. High-temperature NMR results of Janssen *et al.* (*17*) suggest that with increasing temperature, Na^+ ions in the six-membered rings change occupation sites (new minimum energy sites) due to some change in the framework structure of NaA zeolite. The quadrupole parameters of the six-membered Na^+ ions dramatically changed with increasing temperature (20–277°C) (*17*). A possible exchange of Na^+ ions between sites S_2 and S_1 (see Fig. 10) has also been suggested (*18*).

The results of Fig. 2 with NaA could, therefore, be explained based on the above-mentioned structural changes. The effect of temperature is to increase the effective window of the six-membered ring of the sodalite cage by changing the position of Na^+ ions in that window. The decrease in the amount of H_2 encapsulation with increasing temperature in the range 37–200°C for NaX (*1*) may imply that the positions of Na^+ ions at site II in zeolite X have no influence on the passage of H_2 into the sodalite cage, whereas Na^+ ion positions in NaA do restrict movement of H_2 into the sodalite cages of NaA.

The encapsulation results shown in Fig. 3 and Table 3 for Eu/NaA are very informative. The Eu/NaA zeolite gave a similar H_2 TPDiff peak as the NaA zeolite after sorption at 37°C, but with higher amounts of encapsulation (compare Tables 1 and 3). These results suggest that europium ion(s) positions (after dehydration) are likely to affect passage of H_2 in the sodalite cages of zeolite A. It is suggested that a second site for H_2 encapsulation in NaA zeolite exists besides that of the sodalite cage already discussed. The present results (Figs. 1–3) suggest that this second site for H_2 encapsulation is the supercage (α-cage). The Cs/NaA and Ni/NaA encapsulation results discussed next also support this assignment. Hydrogen can diffuse without much difficulty through the eight-membered rings and finally get trapped in the supercages of zeolite A.

The higher uptake of H_2 obtained with Eu/NaA than NaA (Fig. 7, Tables 1 and 3) and the higher diffusion rate in Eu/NaA than in NaA could be explained by a larger effective opening of the eight-membered ring in Eu/NaA than in NaA. As mentioned previously, 3 Na^+ ions/UC. exist at the center of this window in NaA (site S_1, Fig. 10). These ions were found to exchange with other cations (*19*). Therefore, in the present $Eu_{3.2}Na_{2.4}A$ zeolite it appears that some of these Na^+ ions had been exchanged for Eu^{3+} ions. An increase in sorption capacity of other molecules like water and butane when Ca^{2+}, Li^+, K^+, and Rb^+ ions were exchanged for Na^+ ions in zeolite A has been observed (*20, 21, 27*) in analogy to the larger uptakes of H_2 for Eu/NaA.

Our previous H_2 encapsulation results with Eu/NaX (zero H_2 uptake) (*1*) and the present ones with Eu/NaA (non-zero uptake, Fig. 3, Table 3) argue against any blockage of twelve-membered and eight-membered ring of X and A zeolite, respectively, by occluded material that might be present after preparation and heat treatments. These obervations strongly suggest that Eu^{3+} may indeed exchange into 4A zeolite. In addition, the possibility of blockage of 12-membered rings of Eu/NaX zeolite by other europium ions, besides Eu_4O^{+10}, that might be present after dehydration, is unlikely based on the Eu/NaA results of Fig. 3 which conclusively show sorption for this smaller pore zeolite.

(*B*) *H_2 Encapsulation of Cs/NaA and Ni/NaA Zeolites*

When NaA is ion-exchanged with Cs^+ cations, replacement of Na^+ by Cs^+ is believed to occur first at sites S_1 (Fig. 10) until these sites become occupied by three Cs^+ ions (*22, 23*). There are eight Na^+ ions sur-

rounding site S_1 in perfect cubic symmetry, as well as one Na^+ ion at a site opposite to the four-membered rings (site S_3, Fig. 10). To minimize electrostatic repulsion, the latter Na^+ ion may to some extent push the exchangeable Cs^+ ion at site S_1 out of the eight-membered ring plane (*3*).

The present composition of Cs/NaA zeolite lies in the cation site assignment mentioned in the previous paragraph. The decrease in quantity of encapsulated H_2 in Cs/NaA compared to that in NaA after sorption at 37°C (Figs. 1, 2 and 4A–4C) could, therefore, be explained by the smaller effective opening of the eight-membered rings due to the relatively high Cs^+ content. This result also supports the assignment of the H_2 TPDiff peaks in Figs. 1, 3, and of the first peak in Fig. 6 to encapsulation taking place in the α-cage (supercage) of zeolite A.

The H_2 TPDiff result of Fig. 4, curve (C), in relation to that obtained with Eu/NaA (no second peak, T_M = 200°C), indicates that the Cs^+ content in Cs/NaA did not suppress encapsulation of H_2 in the sodalite cage. This result is consistent with the site cation assignment of Cs/NaA given above and the discussion about the cause of H_2 encapsulation following sorption at 200°C in NaA mentioned in the previous section. The effect of degree of Cs^+ exchange in zeolite A on the amount of H_2 encapsulation has been extensively studied by Fraenkel *et al.* (*2–5*) but at pressures in the range 120–134 bar. In their study (*3*) the authors proposed that between 0 and 2.3 Cs^+/U.C., encapsulation of H_2 was restricted only to the sodalite (β-cage) cage of zeolite A. This result is not the same as that found here (Fig. 4, curve (C)). Comparing curves (A)–(C) in Fig. 4 it is clear that some of the encapsulated H_2 is associated with the α-cage (supercage) of zeolite A and the majority is associated with sodalite cages.

Immediately after sorption of hydrogen at 1 atm in our experiments, there is a switch to He to ensure purge of gas phase H_2 followed immediately by temperature-programmed diffusion of hydrogen out of the zeolite. It should be emphasized that the hydrogen encapsulated in the supercages is not evacuated from the zeolite prior to TPDiff experiments. This procedure is different than experiments of Fraenkel *et al.* (*2–5*).

When NaA is ion-exchanged with Ni^{2+} cations and dehydrated, it was found (*24*) that Ni^{2+} ions are concentrated at the centers of the six-membered rings (planar coordinated hexagonal sites) in the α-cages (site S_2, Fig. 10). When sorption was performed at 200°C, encapsulation in the β-cage of Ni/NaA was significantly reduced in comparison to NaA (Fig. 5, curve (C) and Fig. 2, curve (C)). Encapsulation in the α-cage of Ni/NaA after sorption at 37°C did not decrease to the extent observed for the β-cage type of encapsulation (Fig. 5, curves (A) and (B), Table 1). The smaller size of Ni^{2+} ions (0.72 Å) compared to Na^+ ions (0.97 Å) may not be an appropriate explanation for the large decrease of H_2 encapsulation in the β-cages of Ni/NaA compared to NaA. Electrostatic fields created by Ni^{2+} that may affect sorption of H_2 in the β-cages might be appropriate to explain this. A similar explanation was given in the case of Ni/NaX (*1*), where the H_2 TPDiff spectrum was much different from that obtained with NaX zeolite. Migration of Ni^{2+} from site S_2 (Fig. 10) to another site upon H_2 treatment at 200°C, which in turn would increase the effective size of the six-membered rings and allow encapsulation to occur in β-cages, may also be considered. This is consistent with the result of Fig. 5, curve (C) (second peak). In addition, such Ni^{2+} migration does not seem to have affected encapsulation in the α-cage (compare first peak in Fig. 5, curves (A) and (C)).

The result of Fig. 5, curve (C), with Ni/NaA does not seem to correspond to chemisorption of H_2 on Ni^0 after sorption at 200°C. Evidence was given (*25*) that reduction of Ni^{2+} in ion-exchanged zeolites X and Y occurs at temperatures higher than 250°C depending on the Ni^{2+} loading. Reduction

of Ni^{2+} in Ni/NaA at 200°C seems, therefore, unlikely. Attempts to probe the presence of Ni^0 by CO chemisorption, after H_2 treatment at 200°C for 1 h, resulted in no measurable amount of chemisorption for our samples.

(C) H_2 Diffusion in A Zeolites

Further support for assignment of the low T_M (100°C) peak of our TPDiff data to diffusion out of supercages and the high T_M (200°C) peak to diffusion out of sodalite cages is given below.

In order for H_2 to diffuse out of the zeolite it must do so through the large channels that lead into the supercages. For H_2 to diffuse out of sodalite cages there is a larger activation barrier. Thus H_2 inside the sodalite cages must first escape into the supercages and then diffuse out the pores of the zeolite.

The amounts of H_2 diffusing out of the zeolite corresponding to the first peak are substantially larger than those corresponding to the second TPDiff peak for NaA, NiA, and EuA. There is considerably more void volume for supercage sites (755 $Å^3$) than for sodalite sites (155 $Å^3$). Of course, these void volumes are influenced by cation population, however, in most cases there is more room for H_2 encapsulation in supercages than in sodalite cages.

An exception to the generalization of the last paragraph is the CsA system. In this case, Cs^+ ions at this loading block the eight-member rings and severely restrict encapsulation of H_2 in the supercages due to the location of the Cs^+ ions. This blockage also restricts entry to the sodalite cages unless the temperature during encapsulation is substantially raised to (in our studies) 200°C. In this case, both the supercages and sodalite cages encapsulate H_2. However, we believe that the larger intensity TPDiff peak with a T_M near 200°C is due to escape of H_2 from sodalite cages.

For NaA, Na^+ ions block entry of H_2 into the sodalite cages for encapsulation at room temperature. When encapsulation is carried out at 200°C, entrance into the sodalite cages is allowed due to the enhanced vibration of the Na^+ ions, similar to the CsA system. For NiA, Ni^{2+} cations block some of the six-member windows of the sodalite cages. The remaining unexchanged Na^+ ions in the starting material also block entry of H_2 into the sodalite cages. Even at 200°C there is minimal encapsulation of H_2 in the sodalite cages. This may be due to the high charge of the Ni^{2+} ions with concomitant strong binding (less vibration) to the oxygens in the six-membered rings of the sodalite cages.

The shapes and positions of the H_2 TPDiff curves for NaA (Fig. 1) compared to those for Eu/NaA (Fig. 3) and Ni/NaA (Figs. 5A–5C, 1st peak, T_M = 85°C) are similar. These results indicate that diffusion of H_2 encapsulated in the α-cages (supercages) out of the zeolites is similar for all three zeolites. The rate-limiting step may be the successive jumps of H_2 through the eight-membered rings. The small difference (2.4 kcal/mol) in the activation energy of diffusion of H_2 encapsulated in the α-cages of NaA and Eu/NaA, and the site location of Ni^{2+} in Ni/NaA support this idea.

The activation energy for diffusion of H_2 out of the β-cage (sodalite) of NaA (E = 26.0 kcal/mol) agrees with that of 28.5 kcal/mol obtained by Fraenkel (*3*). On the other hand, the present D_o/α^2 value for diffusion out of the sodalite cages of NaA is lower by 3 orders of magnitude than that reported (*3*). The large difference in the D_o/α^2 values for the two types of H_2 encapsulation in NaA found here (3.1×10^3 vs 2.9×10^8 s^{-1}) is also significant. These results indicate that different zeolitic windows are associated with discrete D_o values. In the work of Fraenkel *et al.* (*5*) it was found that D_o was independent of the degree of ion-exchange and the diffusing gas molecule in the Cs/NaA system. Similar behavior was reported by Barrer for Ca-A, Na-A, and K-A zeolites (*26*).

The TPDiff results of Fig. 4 with Cs/NaA are very interesting since they show differ-

ences compared to all the other zeolites (Figs. 1–3 and 5). For H_2 sorption at 37°C there is a broadening in the TPDiff spectra (Fig. 4, curves (A) and (B)), and this becomes more pronounced at higher sorption temperatures (Fig. 4, curve (C)). For the latter case, the two types of H_2 encapsulation cannot be resolved. This behavior may be related to the different positions and sizes of Cs^+ ions in Cs/NaA zeolite compared to those of corresponding ions in NaA, Ni/NaA and Eu/NaA. Diffusion of H_2 out of the supercage appears to be more difficult in the Cs/NaA case than in the other zeolites. The small quantities of H_2 encapsulation for Cs/NaA and Ni/NaA, and the overlap of peaks (two types of encapsulation) for the former zeolite (Fig. 4), did not permit reliable evaluation of kinetic parameters (E, D_0/α^2 and D/α^2) as with NaA and Eu/NaA zeolites.

Finally, our present and previous work (*1*) showed that H_2 sorption (encapsulation) at 1 atm in zeolites A and X can be effectively used to study and understand the role various cations in zeolites might play on diffusion processes.

CONCLUSIONS

1. Two sites of encapsulation of molecular H_2 in zeolite NaA were identified following sorption at 1 atm. The population of these two sites (α-cage and β-cage) depends on the temperature of sorption.

2. The amount of H_2 encapsulation in these two sites is small, 1.5 and 2.0 μmol/g for the β-cage and α-cage, respectively, and no more than 5% of the chemisorbed H_2 that might be expected from a typical metal-loaded zeolite system. The diffusion of molecular H_2 into the α-cage of zeolite A at 37°C and 1 atm H_2 pressure is slow, where about 24 h is required to achieve an equilibrium state.

3. Passage of molecular H_2 out of the α-cage is controlled by diffusion through the eight-membered rings, whereas diffusion out of the β-cage occurs via the six-membered rings. The activation energies and diffusivities for these two types of diffusion processes are much different, allowing discrete diffusion properties of each zeolite window to be probed.

ACKNOWLEDGMENTS

The support of the Department of Energy, Office of Basic Energy Sciences, Division of Chemical Sciences is gratefully acknowledged. We thank Dr. Lennox E. Iton for helpful discussions regarding this research.

REFERENCES

1. Efstathiou, A. M., Suib, S. L., and Bennett, C. O., *J. Catal.* **123,** 456 (1990).
2. Fraenkel, D., and Shabtai, J., *J. Am. Chem. Soc.* **99,** 7074 (1977).
3. Fraenkel, D., *J. Chem. Soc. Faraday Trans. 1* **77,** 2029 (1981).
4. Fraenkel, D., *J. Chem. Soc. Faraday Trans. 1* **77,** 2041 (1981).
5. Fraenkel, D., Ittah, B., and Levy, M., *J. Chem. Soc. Faraday Trans. 1* **84**(6), 1835 (1988).
6. Morrison, T. I., Reis, A. H., Gebert, E., Iton, L. E., Stucky, G. D., and Suib, S. L., *J. Chem. Phys.* **72,** 6276 (1980).
7. Suib, S. L., McMahon, K. C., Tau, L. M., and Bennett, C. O., *J. Catal.* **89,** 20 (1984).
8. Stockwell, D. M., Chung, J. S., and Bennett, C. O., *J. Catal.* **112,** 135 (1988).
9. Fraenkel, D., and Levy, A., *J. Chem. Soc. Faraday Trans. 1* **84**(6), 1817 (1988).
10. Crank, J., "The Mathematics of Diffusion." Clarendon Press, Oxford, 1956.
11. Eberly, P. E., Jr., *in* "Zeolite Chemistry and Catalysis" (J. Rabo, Ed.), Vol. 171, pp. 392–436, ACS Monography. ACS, Washington, DC, 1976.
12. Olson, D. H., Kokotailo, G. T., and Charnell, J. R., *J. Colloid Interface Sci.* **28**(2), 305 (1968).
13. Bartlett, J. R., Cooney, R. P., and Kydd, R. A., *J. Catal.* **114,** 58 (1988).
14. Breck, D. W., "Zeolite Molecular Sieves: Structure Chemistry and Use." Wiley, New York, 1974.
15. Reed, T. B., and Breck, D. W., *J. Am. Chem. Soc.* **78,** 5972 (1956).
16. Rabo, J. A., Jr., *in* "Zeolite Chemistry and Catalysis" (J. Rabo, Ed.), Vol. 171, Ch. 1, ACS Monograph, ACS, Washington, DC, 1976.
17. Janssen, R., Tijink, G. A. H., Veeman, W. S., Maesen, Th. L. M., and van Lent, J. F., *J. Phys. Chem.* **93,** 899 (1989).
18. Jeener, J., Meier, B. H., Bachmann, P., and Ernst, R. R., *J. Chem. Phys.* **71,** 4546 (1979).
19. Kevan, L., and Lee, H., *J. Phys. Chem.* **90,** 5776 (1986).

20. Ohgushi, T., Yusa, A., and Takaishi, T., *J. Chem. Soc. Faraday Trans. 1* **73,** 613 (1977).
21. Tsitsishvili, G. V., and Andronikashvili, T. G., *Adv. Chem. Ser.* **102,** 217 (1971).
22. Pluth, J. J., and Smith, J. V., *J. Am. Chem. Soc.* **102,** 4704 (1980).
23. Subramanian, V., and Seff, K., *J. Phys. Chem.* **84,** 2928 (1980).
24. Klier, K., and Ralek, M., *J. Phys. Chem. Solids* **29,** 951 (1968).
25. Coughlan, B., and Keane, M. A., *J. Catal.* **123,** 364 (1990).
26. Barrer, R. M., "Zeolites and Clay Minerals," p. 292. Academic Press, London, 1978.
27. Ruthven, D. M., "Principles of Adsorption and Adsorption Processes," Chap. 5. Wiley, New York, 1984.
28. (a) Iton, L. E., Suib, S. L., Stucky, G. D., *Bull. Magn. Reson.* **2,** 174 (1981). (b) Iton, L. E., Brodbeck, C. M., Suib, S. L., Stucky, G. D., *J. Chem. Phys.* **79,** 1185 (1983).
29. Suib, S. L., Zerger, R. P., Stucky, G. D., Emberson, R. M., Debrunner, P. G., and Iton, L. E., *Inorg. Chem.* **19,** 1858 (1980).